MASP-1, a Promiscuous Complement Protease: Structure of Its Catalytic Region Reveals the Basis of Its Broad Specificity[1]

József Dobó,[2,3]* Veronika Harmat,[3†] László Beinrohr,* Edina Sebestyén,* Péter Závodszky,* and Péter Gál[2]*

Mannose-binding lectin (MBL)-associated serine protease (MASP)-1 is an abundant component of the lectin pathway of complement. The related enzyme, MASP-2 is capable of activating the complement cascade alone. Though the concentration of MASP-1 far exceeds that of MASP-2, only a supporting role of MASP-1 has been identified regarding lectin pathway activation. Several non-complement substrates, like fibrinogen and factor XIII, have also been reported. MASP-1 belongs to the C1r/C1s/MASP family of modular serine proteases; however, its serine protease domain is evolutionary different. We have determined the crystal structure of the catalytic region of active MASP-1 and refined it to 2.55 Å resolution. Unusual features of the structure are an internal salt bridge (similar to one in factor D) between the S1 Asp189 and Arg224, and a very long 60-loop. The functional and evolutionary differences between MASP-1 and the other members of the C1r/C1s/MASP family are reflected in the crystal structure. Structural comparison of the protease domains revealed that the substrate binding groove of MASP-1 is wide and resembles that of trypsin rather than early complement proteases explaining its relaxed specificity. Also, MASP-1's multifunctional behavior as both a complement and a coagulation enzyme is in accordance with our observation that antithrombin in the presence of heparin is a more potent inhibitor of MASP-1 than C1 inhibitor. Overall, MASP-1 behaves as a promiscuous protease. The structure shows that its substrate binding groove is accessible; however, its reactivity could be modulated by an unusually large 60-loop and an internal salt bridge involving the S1 Asp. *The Journal of Immunology,* **2009, 183: 1207–1214.**

The complement system is an integral part of the immune system. It plays an essential role in both the innate and adaptive immune responses. Activation of the complement system culminates in the destruction of invading pathogens and elimination of altered host structures (e.g., apoptotic cells) and contributes to the development of inflammation via stimulation of the cellular elements of the immune system (1). The complement system is a proteolytic cascade system that can be activated through three different routes: the classical, the lectin, and the alternative pathway. The lectin pathway of complement can directly recognize the pathogen microorganisms through lectin molecules that can bind to the carbohydrate structures on foreign surfaces. Mannose-binding lectin (MBL)[4] and ficolins (L-/H- and M-ficolin) are pattern-recognition molecules that form the recognition subunits of the lectin activation pathway (2). When these molecules bind to the foreign structures, the associated serine protease zymogens (MBL-associated serine proteases (MASPs)) become activated. Up to now, three kinds of MASPs have been identified, denoted MASP-1, MASP-2, and MASP-3. MASP-2 is the only MBL-associated protease that can efficiently activate the complement cascade alone (3). MASP-2, like C1s in the classical pathway, can cleave C4 and C2 that form the C3-convertase complex (C4b2a) (4, 5). The function of MASP-3 is unclear. It has been suggested that MASP-3 can down-regulate the activity of MASP-2 because they are competing for the same MBL molecules (6). The most abundant MASP in the serum is MASP-1. Its serum concentration is roughly ten times higher than that of MASP-2 (~70 and ~5 nM, respectively) (7, 8). MASP-1, like MASP-2, can autoactivate; however, it cannot initiate the formation of the C3-convertase because it can cleave only C2 with sufficient efficiency, and it is practically inactive toward C4. Several lines of evidence suggest that MASP-1 can support the C3-convertase-generating activity of MASP-2 by increasing the rate of C2 cleavage (9, 10). This could explain why every C4b deposited by the MBL-MASPs complex can form C4b2a convertase, whereas only one of four C4b deposited by the classical pathway C1 complex can do the same (11). It was also suggested that MASP-1 can facilitate the activation of MASP-2 (12). Because MASP-2 alone can readily autoactivate (13), the relevance of this reaction is questionable. It has also been shown that MASP-1 can cleave C3 with very low efficiency (5, 14). This slow C3 cleavage could be due to the hydrolysis of C3, because MASP-1 cleaves hydrolyzed C3 (C3i) with ~20-fold higher (but still low) efficiency than native C3 (4). The physiological relevance of this C3 cleavage is therefore questionable. Studies with synthetic peptide substrates showed that MASP-1, like

*Institute of Enzymology, Biological Research Center, Hungarian Academy of Sciences, Budapest, Hungary; and †Protein Modeling Group, Hungarian Academy of Sciences, and Laboratory of Structural Chemistry and Biology, Institute of Chemistry, Eötvös Loránd University, Budapest, Hungary

Received for publication April 8, 2009. Accepted for publication May 15, 2009.

The costs of publication of this article were defrayed in part by the payment of page charges. This article must therefore be hereby marked *advertisement* in accordance with 18 U.S.C. Section 1734 solely to indicate this fact.

[1] Data from the European Community (Research Infrastructure Action under the FP6 "Structuring the European Research Area Specific Programme" to the EMBL Hamburg Outstation, Contract Number RII3-CT-2004-506008). This work was supported by the Ányos Jedlik Grant NKFP_07_1-MASPOK07 of the Hungarian National Office for Research and Technology, and by the Hungarian Scientific Research Fund Grants NK77978, NI61915, K72973, F67937, and NK67800.

[2] Address correspondence and reprint requests to Dr. J. Dobó or Dr. P. Gál, Institute of Enzymology, Biological Research Center, Hungarian Academy of Sciences, Karolina út 29, H-1113, Budapest, Hungary. E-mail address: dobo@enzim.hu or gal@enzim.hu

[3] J.D. and V.H. contributed equally to this work.

[4] Abbreviations used in this paper: MBL, mannose-binding lectin; AT, antithrombin; C1-inh, C1-inhibitor; CCP, complement control protein; CUB, C1r/C1s, sea urchin Uegf and bone morphogenetic protein-1; EGF, epidermal growth factor; IR, ischemia reperfusion; MASP, MBL-associated serine protease; SP, serine protease.

thrombin, has extreme Arg preference at the P1 position (15). It was also demonstrated that MASP-1 is capable of cleaving fibrinogen and factor XIII, although less efficiently than thrombin does (16, 17). This activity of MASP-1 could represent an ancient type of innate immunity, well known in lower organisms: the localized coagulation. Molecular evolutionary studies also proved that MASP-1 is a more ancient type of protease than the other early complement proteases: C1r, C1s of the classical, and MASP-2 and MASP-3 of the lectin pathway (18). C1r, C1s, MASP-1, MASP-2, and MASP-3 form a family of mosaic serine proteases with identical domain organization. These molecules consist of six domains. At the N-terminal there is a C1r/C1s, sea urchin Uegf, and bone morphogenetic protein-1 (CUB) domain followed by an EGF-like module and a second CUB domain. This noncatalytic N-terminal region of the molecule is responsible for the dimerization and for interaction with MBL. In the C-terminal half of the molecules, a tandem repeat of complement control protein (CCP) modules precedes the trypsin-like serine protease (SP) domain.

An intact complement system is essential in preventing infections and maintaining the internal immune homeostasis; however, uncontrolled activation of the system can result in host tissue damage and inflammation (19). An important example is ischemia-reperfusion (IR) injury, in which restoration of blood flow after transient ischemic condition results in serious tissue damage (e.g., postmyocardial IR injury). Increasing evidence shows that the lectin pathway plays a critical role in IR injury and targeting the proteases of the lectin pathway might be effective in reducing the tissue damage caused by IR injury (20).

During recent years, there has been great progress in the structural biology of the complement proteases of both the classical and the lectin pathway. The structures of the catalytic fragments of C1r (21–23), C1s (24), and MASP-2 (13, 25) have been determined. The structure of the CUB1-epidermal growth factor (EGF) fragment of C1s (26) and the CUB1-EGF-CUB2 fragment of rat MASP-2 (27) is also known. These structures provided insights into the structural background of MBL-binding, catalytic activity, and substrate specificity of these proteases and, in the case of C1r and MASP-2, they provided information about the mechanism of autoactivation. Recently, the crystal structure of the CUB1-EGF-CUB2 fragment of MASP-1/3 has been solved (28). Up to now there has not been any structural information available about the catalytic region of MASP-1. In this study we have determined the structure of the CCP1-CCP2-SP catalytic fragment of MASP-1. The structure opens up the way for designing specific inhibitors against this protease, and helped us to explain the unusual broad substrate specificity of MASP-1 providing hints about its physiological role.

Materials and Methods

Expression, purification, and crystallization of rMASP-1

MASP-1 CCP1-CCP2-SP (rMASP-1) was expressed in *Escherichia coli* the form of inclusion bodies. The construct contains an Ala-Ser-Met-Thr expression-enhancing tag at the N terminus, followed by the Gly298-Asn699 fragment of human MASP-1 (the numbering includes the signal peptide). The protein was expressed as described earlier (4). Details of the refolding, purification, and crystallization were published elsewhere (29). It is important to note that rMASP-1 autoactivates during the refolding procedure. The crystal, from which the best dataset was collected, was obtained as follows: 2 μl rMASP-1 at 13 mg ml^{-1} in 50 mM NaCl, 5 mM Tris, 0.5 mM EDTA, 20 mM benzamidine-HCl, pH 8.8, was mixed with 2 μl of reservoir solution that contained 11% (w/v) PEG3350 and 0.1 M MES, pH 6.5, and crystallized by the vapor-diffusion hanging-drop method. The crystal was gradually soaked into reservoir buffer supplemented with 5, 10, 15, and 20% (v/v) glycerol, and flash-cooled in liquid nitrogen mounted on nylon loops (Hampton Research).

Table I. *Data collection and refinement statistics*

	rMASP-1[a]
Crystal parameters	
Space group	$P2_12_12_1$
Cell constants (Å)	a = 68.418, b = 70.412, c = 121.413
Data quality	
Resolution range (last resolution shell)	45.98–2.55 Å (2.616–2.55 Å)
R_{meas}[b]	10.4 (51.5)
Completeness	97.9% (97.4%)
No. of observed/unique reflections	114,297/19,349 (6216/1066)
$I/\sigma(I)$	15.96 (4.35)
Refinement residuals	
R	0.231
R_{free}[c]	0.278
Model quality	
R.m.s.[d] bond lengths (Å)	0.007
R.m.s. bond angles (°)	1.163
R.m.s. general planes (Å)	0.003
Ramachandran plot: residues in core/allowed/disallowed regions	297/37/1
Model contents	
Protein residues	398
Glycerol molecules/water molecules	2/90
No. of atoms	3,196
Residues in dual conformations	5
Residues with disordered side chains	20
Disordered residues	11

[a] Values in parentheses correspond to the highest resolution shell (2.616–2.55 Å).
[b] $R_{meas} = \{\Sigma_h(n/(n-1))^{0.5}\ \Sigma_j|I_{hj} - \langle I_h\rangle|\}/(\Sigma_{hj}\ I_{hj})$, with $\langle I_h\rangle = (\Sigma_j\ I_{hj})/n_j$.
[c] A percentage (5.1) of the reflections were used in a test set for monitoring the refinement process.
[d] R.m.s. = root mean square.

Data collection, structure determination, and refinement

Data collection was conducted using synchrotron radiation (EMBL beamline X11 at DESY, Hamburg) at 100 K (wavelength 0.08148 nm, 165 mm MarCCD detector). Data reduction was conducted using the XDS package (30). The phase problem was solved by molecular replacement with the MOLREP program (31) using a SP domain of a lower resolution chimerical structure containing the SP domain of MASP-1 (E. Sebestyen, V. Harmat, J. Dobó, P. Závodszky, P. Gál, unpublished data) and CCP1 and CCP2 modules of MASP-2 (Protein Data Bank (PDB) entry 1zjk) (13) as models. Manual model building and automated search for water molecules were conducted using the Coot program (32). Refmac5 (33) of the CCP4 program suite (Collaborative Computational Project, Number 4, 1994) was used for refinement. TLS refinement was performed using two TLS groups: one for the CCP1-CCP2 part of the molecule, and the other for the SP domain. Bulk solvent scaling was applied. Hydrogen atoms were generated in the riding positions. The stereochemistry of the structure was checked with the PROCHECK program (34). Data reduction and refinement statistics are shown in Table I. The atomic coordinates and structure factors were deposited in the Protein Data Bank (http://www.rcsb.org/pdb) with accession no. 3gov.

Purification of the R504Q variant of rMASP-1

The wild-type enzyme was purified in the presence of benzamidine for crystallization to avoid autolysis of rMASP-1 (4). Because benzamidine could disturb the kinetic measurements, for this purpose we chose the autolysis resistant R504Q mutant that can be purified undegraded in the absence benzamidine. This mutant has the same enzymatic properties on peptide substrates as the wild-type enzyme. A one-step simplified protocol was used for the purification of R504Q rMASP-1, which was expressed and refolded as the wild-type enzyme (29). Benzamidine was omitted during purification, as it could interfere with the kinetic assays. Five hundred milliliters of the refolding mixture (200 mg L^{-1} R504Q rMASP-1, 0.3 M Arg, 1 M NaCl, 50 mM Tris, 5 mM EDTA, 4 mM glutathione, 4 mM oxidized glutathione, pH 9.4) was dialyzed for 2 days against 2 × 10 l of 1 mM Tris, 0.5 mM EDTA, pH 8.8 with one exchange after day 1, then it was applied to a 20 ml Source 30Q (GE Healthcare) column equilibrated with 5 mM Tris, 0.5 mM EDTA, pH 8.8, buffer and eluted with a 0–200 mM NaCl gradient in 5 mM Tris, 0.5 mM EDTA, pH 8.8 buffer in 25-column volumes. Fractions were assayed for activity (see conditions in the next section) and purity by SDS-PAGE, then selected fractions were combined, concentrated to ~3 mg ml^{-1} on spin concentrators, and stored at −70°C. The molar concentration of R504Q rMASP-1 was calculated based on the extinction coefficient ε = 1.54 ml mg^{-1} cm^{-1}, and a molecular mass of 45.5 kDa.

Inhibition assays

Lyophilized C1-inhibitor (C1-inh) (Berinert P; CSL Behring) was dissolved and gel-filtrated on a Sephadex G-25 column (GE Healthcare) in 50 mM HEPES, 140 mM NaCl, 0.1 mM EDTA, pH 7.4. buffer. The C1-inh containing fractions were concentrated to ~0.9 mg ml^{-1} and stored at −70°C. The molar concentration of C1-inh was calculated based on the extinction coefficient $\varepsilon = 0.382$ ml mg^{-1} cm^{-1}, and a molecular mass of 71 kDa.

Antithrombin (AT) was prepared from pooled, outdated human plasma. Heparin Sepharose 6 Fast Flow column (GE Healthcare) was equilibrated with 20 mM HEPES, 100 mM NaCl, 0.1 mM EDTA, pH 7.4. The plasma was loaded onto the column, then washed with equilibration buffer. AT was eluted using a 20-column-volume linear salt gradient (0.1 M to 2 M NaCl). AT containing fractions were then gel-filtrated, concentrated, and stored as described for C1-inh. The molar concentration of AT was calculated based on the extinction coefficient $\varepsilon = 0.65$ ml mg^{-1} cm^{-1}, and a molecular mass of 58 kDa.

The activity and inhibition of R504Q rMASP-1 was assayed in 50 mM HEPES, 140 mM NaCl, 0.1 mM EDTA, pH 7.4 buffer, using the substrate VLR-pNA (V6258; Sigma-Aldrich) at 200 μM concentration. The final enzyme concentration was 10 nM. C1-inh was used at 0 or 200-2000 nM and AT at 0 or 200-2000 nM, whereas heparin was applied at 0 or 0.1–1000 μg ml^{-1} final concentration.

The second order rate constants of inhibition (k_{ass}) were determined under pseudo-first-order conditions as described (35, 36). Data were fitted by nonlinear regression using the $A = a - b \times e^{-k_{obs} \times t} + c \times t$ equation, where A is the absorbance; a, b, and c are fitting parameters; and k_{obs} is the observed association rate constant. The second order rate constants (k_a) were approximated as $k_a = k_{obs}/[I]_0$, where $[I]_0$ is the serpin concentration, because in the used-inhibitor range, k_{obs} was proportional with the inhibitor concentration (37).

Results

The overall structure

The recombinant catalytic fragment of human MASP-1 (Fig. 1*A*), which is composed of the first and second CCP domains and the SP domain, was produced in *E. coli*, refolded from inclusion bodies and crystallized. The construct (406 residues) contains an Ala-Ser-Met-Thr tag at the N terminus followed by the Gly298-Asn699 segment of MASP-1. Details of the crystallization are described elsewhere (29). The structure was solved by molecular replacement and refined to a 2.55 Å resolution (Table I). Overall, 398 of 402 MASP-1 residues could be built into the electron density map. In the N-terminal tag, four residues of the activation loop of the SP domain and 20 side chains spread in loop regions were disordered in the crystal. Interestingly, benzamidine, which was present in the crystallization liquor to protect the enzyme from autodegradation is not seen in the structure. Possibly benzamidine diffused away during a procedure when the crystal was soaked in cryo solutions containing glycerol at incrementally increasing concentrations, or the internal salt bridge (discussed later) between the S1 Asp640 (c189) and Arg677 (c224) may be responsible for this effect. It should be noted here that the numbering in the text follows the precursor MASP-1 numbering for MASP-1 and chymotrypsin numbering is indicated in parenthesis denoted with "c" when necessary for easier comparison. For other proteases chymotrypsin numbering is used throughout the text.

Recombinant MASP-1 CCP1-CCP2-SP (rMASP-1) has essentially the same fold and overall shape as the C1s/C1r/MASP-2 structures containing the two CCP domains concatenated in a rod-like structure attached to the globular SP domain (Fig. 1*B*). The domain orientation at the CCP2/SP junction shows minor differences from that of other structures, which is in line with the limited flexibility of this region among these proteases. Comparison of the CCP2/SP interface of MASP-1, MASP-2, C1r, and C1s revealed conserved contacts between the Pro-Tyr-Tyr motif (400–402) of the CCP2 domain, the Pro-Val-Cys linker region (434–436), and the SP domain, although in the contact region of the SP domain

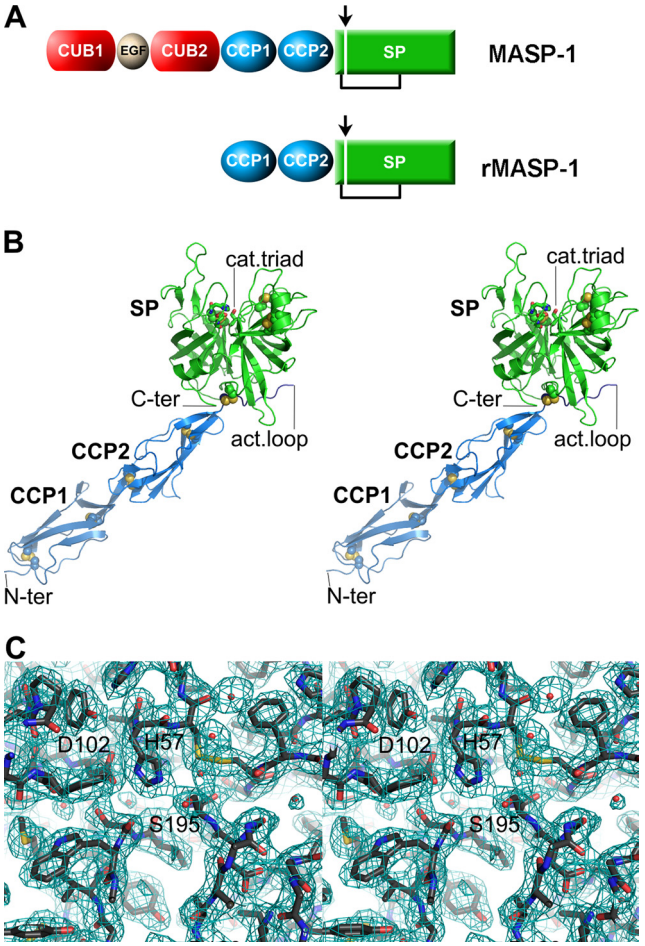

FIGURE 1. Overall structure of active MASP-1 CCP1-CCP2-SP (rMASP-1). *A*, Schematic representation of the domain structure of MASP-1 and the expressed fragment (rMASP-1). Related proteins C1r, C1s, MASP-2, and MASP-3 share the same domain organization as MASP-1. *B*, Overall structure of rMASP-1 (PDB id: 3gov). Disulphide bridges and the catalytic triad are shown as spheres and sticks, respectively. *C*, σ_A scaled $2F_o$-F_c electron density map of the active site contoured at 1.0 σ level. The catalytic triad is labeled using chymotrypsin numbering.

Pro570 is the only conserved residue. A novel element of the MASP-1 contact region is the salt bridge between the C-terminal Asn699 carboxyl group and Lys403 of the CCP2 domain. The C terminus is stabilized in an extended conformation by hydrogen bonds of Asn699 and hydrophobic contacts of Val697 to the body of the SP domain. Comparison of the CCP1/CCP2 domain junction of known structures MASP-1, MASP-2, and C1r reveals many structurally conserved main chain hydrogen bonds and hydrophobic contacts, allowing a minor bend at the domain border. After superimposing the CCP2 domains of MASP-1, MASP-2 (PDB ID: 1zjk), and C1r (PDB ID: 1qy0), the distance of the N-terminal Cys301 Cα in the CCP1 domain is 6.4 and 9.8 Å apart from the Cys in equivalent position in MASP-2, and C1r, respectively.

The overall fold of the SP domain resembles that of other proteases of the chymotrypsin family. The residues of the active site (Fig. 1*C*), as well as the S1 binding site, are in canonical conformations. Unique features of the MASP-1 SP domain are described in detail below.

Structure of the SP domain shows an open active site

Comparison of the SP domain with the structures of human MASP-2, C1r, C1s, thrombin, and bovine trypsin reveals that,

except for the variable loops surrounding the substrate binding region, there are two interesting differences in the conformation. First, the region 575–580 (c107–112) is extended, similarly to that of trypsin, though it lacks the disulfide bridge. In contrast, MASP-2, C1r, C1s, and thrombin show helical conformation in this region. Second, the helix of the C-terminal region is about one turn shorter than that of related complement proteases, caused by the unusual interaction of the C terminus with the CCP2 domain.

To explore the structural basis of the substrate selectivity of MASP-1, which is unusually wide compared with related complement proteases, we compared the substrate binding region of the structure with other selected serine proteases. These enzymes have common substrates with MASP-1 (C1r, C1s, MASP-2, and thrombin), and additionally bovine trypsin was included as a reference structure with wide substrate selectivity. The surface topology of MASP-1 resembles that of trypsin, rather than those of enzymes with restricted substrate specificity (C1r, C1s, MASP-2, and thrombin). The substrate-binding groove is wide and exposed. Surface representation near the S1 site (Fig. 2) shows bulky loop regions bending above the substrate binding site in the case of C1r, C1s, and MASP-2, while the enzyme surface of MASP-1 and trypsin is more exposed and smoother at this region. At the border of the S1-S1′ sites, the bulky c192 residue narrows the substrate binding groove in the compared enzymes (in Fig. 2, the middle of the groove, lower side). In contrast, Ala643 in MASP-1 makes the substrate binding site more accessible.

Conformation and length of the loops surrounding the substrate binding region are different even in the case of enzymes with similar substrate specificity (Fig. 3*A*). The most striking feature of the S1-S3 side of the substrate binding region of MASP-1 is the exceptionally long loop B (38), which is also called the 60-loop. This loop contributes highly in the specificity of thrombin containing a cluster of aromatic residues folding over the P2 residue of the substrate. Loop B of MASP-1 is even longer and is loosely packed in a hydrophobic patch of the enzyme surface with seven hydrophobic residues turned inside, while its seven charged residues are solvent exposed. The distribution of stabilizing hydrogen bonds in Loop B suggest that it has kink regions, making possible its bending toward the substrate peptide and interaction of Leu496, Pro498, and Pro501 side chains and a small hydrophobic P2 residue. On the other side of the S1-S3 region, backbone conformation of Loop 2 is similar among the enzymes compared, but this loop holds Arg677 (c224) of MASP-1, which is discussed later in detail. The flexible Loop C closes the substrate binding groove on this side.

On the S1′-S3′ side of the substrate binding region, even higher conformation variability was detected among the complement proteases. This region is significantly more accessible in MASP-1 and trypsin than in other complement proteases or thrombin, contributing to the less restricted substrate specificity. Loop A shields the substrate binding groove at its C-terminal end in all related complement proteases and thrombin. Moreover, Loop D and Loop B restrict accessibility in the case of MASP-2 and thrombin, respectively.

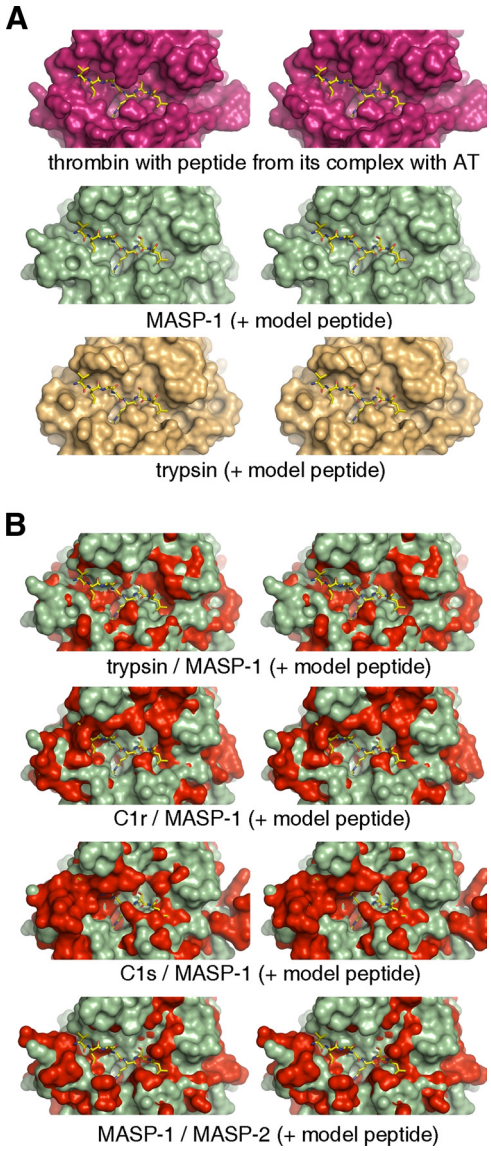

FIGURE 2. The substrate binding groove of MASP-1 is highly accessible. *A*, Surface stereo representations of thrombin (PDB id: 1tb6), MASP-1 (PDB id: 3gov), and trypsin (PDB id: 1k9o) shown near the substrate binding site. The P5-P2′ peptide from AT bound to the thrombin structure is shown as sticks. This model peptide from the thrombin structure fits quite smoothly into the substrate binding groove of both MASP-1 and trypsin. *B*, Surface stereo representation of the structure of MASP-1 (green) overlaid with trypsin, C1r (PDB id: 2qy0), C1s (PDB id: 1elv), or MASP-2 (PDB id: 1q3x) (all red) shown near the substrate binding site. The model peptide (from 1tb6) is placed into the substrate binding groove for better orientation. MASP-1 has a broad cleft at the substrate biding site, which accommodates the model peptide easily. In this respect it is more similar to trypsin than to the other depicted proteases with the same domain organization as MASP-1, which have protrusions that collide with the model peptide.

The internal salt bridge involving the S1 Asp

The most surprising feature of the SP domain of MASP-1 is that the side chain of Arg677 (c224) is rotated toward the Asp640 (c189, which is responsible for primary substrate specificity in the chymotrypsin family) and forms a salt bridge (Fig. 3*B*). This interaction competes with the S1-P1 interaction upon substrate binding. Comparison with the structures of related complement proteases, thrombin, and trypsin reveals a possible way of concerted or induced rotation of side chains, resulting in releasing Asp640 from its salt bridge with Arg677. Loop 2 holding Arg677 is of equal length and similar conformation in MASP-1, MASP-2, thrombin, and trypsin. Loop 2 of C1r and C1s is shorter and it is impossible that any side chain of Loop 2 blocks the S1 Asp. In thrombin and trypsin, a positively charged residue Lys224 is in equal position to that of Arg677. Lys224 side chain of thrombin is stabilized in a noninhibiting position by Glu217, which is in equal position with Asp670 of MASP-1. A c224-c217 salt bridge can also be formed in MASP-1 by rotation of Asp670 (c217) side chain and breaking its salt bridge with Loop 3 (Lys623). Upon substrate

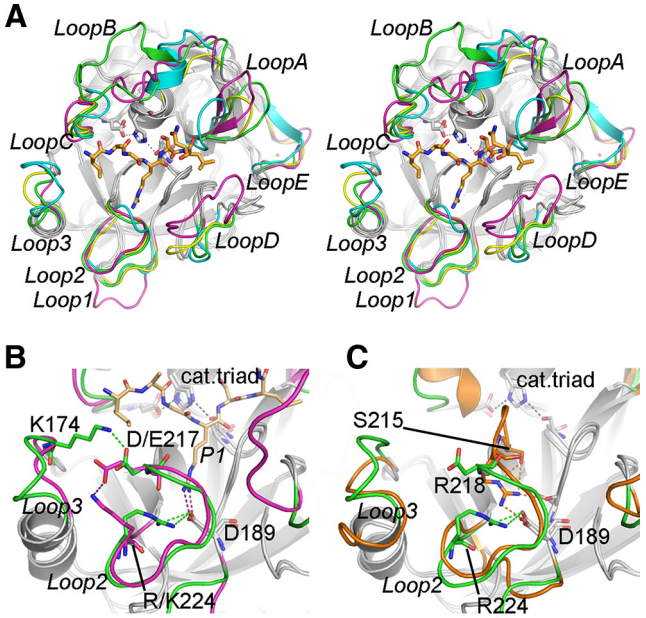

FIGURE 3. Conformation of loop regions building up the substrate binding groove. *A*, Comparison of loops surrounding the active site of MASP-1 (green; PDB id: 3gov) compared with those of MASP-2 (cyan; PDB id: 1q3x), thrombin (magenta; PDB id: 1tb6), and bovine trypsin (yellow; PDB id: 3btk). The P4-P3′ heptapeptide part of AT bound in the thrombin structure is shown in light orange as reference for a bound substrate/inhibitor. Regions with similar backbone conformations are colored gray, with the catalytic triad as sticks. Loops are labeled according Perona and Craik (38). *B*, Blow-up of the substrate specificity pocket using chymotrypsin numbering. An unusual ion pair (Asp640/Arg677, c189/c224) formed by the specificity determinant aspartate of MASP-1 (green) is likely to lower its activity. The c189 aspartate can be liberated from the salt bridge by concerted rotation of side chains c224 and c217 (Arg677 and Asp670) induced by the substrate P1 residue or by turning the c174 (Lys623) side chain. The resulting salt bridge pattern, similar to that of thrombin (magenta), is favorable for accommodating the substrate. *C*, In factor D (orange; PDB id: 1dsu), Asp189 and Arg218 form a salt bridge. In MASP-1 (green), binding of the substrate arginine can be promoted simply by side chain rotation of some residues. In contrast, the complete rearrangement of region 214–218 shielding the entrance of the pocket is crucial in factor D.

binding and formation of the S1-P1 salt bridge, breakage of the salt bridge Arg677-Asp640 is induced, presumably followed by a domino effect, i.e., the re-organization of the ion pair network in a thrombin-like manner. The domino effect and breakage of the salt bridge with Lys623 can possibly be allosterically promoted by changing the conformation of Loop 3 and turning the Lys623 side chain out by interaction with a protein substrate.

In Factor D, the specificity-determinant Asp189 is blocked by a salt bridge (Arg218). This enzyme is in functionally inactive conformation with several distortions in the active site and substrate binding region (39). Comparison of MASP-1 and factor D structures is shown in Fig. 3*C*. In factor D, the S1 pocket is narrowed by Loop 2 (self-inhibitory loop) holding Arg218 and a major rearrangement of the S1 region is needed to make it accessible for the substrate. Loop 2 is involved in the conformational switch, ensuring the high specificity of factor D toward its only macromolecular substrate, C3b-bound factor B. In contrast, in MASP-1 the S1 pocket and the c189 Asp is freely accessible suggesting, that the role of the c189-c224 salt bridge is only the modulation of activity and does not restrict the specificity. In summary, the unusual conformation of Arg677 is likely to play a role in the lower activity of MASP-1 compared with trypsin.

Table II. *Second-order association rate constants (k_a) of reactions with C1-inh and AT in the presence and absence of heparin*

Protease	Inhibitor	Heparin	$k_a/M^{-1}s^{-1}$	Reference
rMASP-1	C1-inh	−	$6.2 \pm 1.0 \times 10^{3}$[c]	This paper
		+[a]	$6.7 \pm 0.7 \times 10^{3}$[c]	This paper
rMASP-1	AT	−	$1.4 \pm 0.1 \times 10^{3}$[c]	This paper
		+[a]	$4.0 \pm 0.2 \times 10^{4}$[c]	This paper
Thrombin	AT	−	$8.7 \pm 0.1 \times 10^{3}$[c]	41
		+[b]	$4.0 \pm 0.4 \times 10^{7}$[c]	42
rMASP-2	C1-inh	−	$2.2 \pm 0.2 \times 10^{7}$[d]	35

[a] Unfractionated heparin, 50 μg ml^{-1}.
[b] High affinity heparin, ~0.8 μg ml^{-1}.
[c] Measured at 25° C.
[d] Measured at 37° C.

Inhibition by C1-inh and AT in the presence and absence of heparin

Many studies confirmed that C1-inh is a physiological inhibitor of MASP-1 (4, 5, 14, 40). In contrast, only one report showed that AT inhibits MASP-1, but only in the presence of heparin (15). Because of the discussed dual role of MASP-1, both in complement and coagulation, we undertook to quantitatively examine the reaction between rMASP-1 and AT in the absence and presence of different concentrations of heparin, and compared it with the rMASP-1/C1-inh reaction and data presented in the literature (35, 41, 42) regarding the thrombin/AT and rMASP-2/C1-inh reaction (Table II). We found that AT was the fastest inhibitor of rMASP-1 in the presence of heparin, and in contrast to Presanis et al. (15), the reaction took place in the absence of heparin as well, although without heparin AT inhibited rMASP-1 slower than C1-inh did. The second order association rate constant (k_{ass}) of the rMASP-1/AT reaction was enhanced by ~30-fold in the presence of 50 μg ml^{-1} heparin. The observed rate is the fastest rate reported so far for MASP-1 inhibition by a natural inhibitor. Our results can be summarized by the following scheme:

$$k_{ass,AT} < k_{ass,C1\text{-}inh} = k_{ass,C1\text{-}inh+heparin} \ll k_{ass,AT+heparin}$$

The heparin concentration dependence of the rate constant of the rMASP-1/AT reaction was examined at 200 nM AT and in the 0.1–1000 μg ml^{-1} unfractionated heparin range (Fig. 4). The lack of a bell-shaped curve is similar to the one observed to the fXa/AT/heparin reaction (42), and indicates that the heparin activation is likely to be mainly allosteric. Heparin accelerates the thrombin/AT reaction differently. The so-called bridging or template mechanism is characterized by a bell-shaped curve (43), indicating a binding site on both the protease and the serpin for heparin.

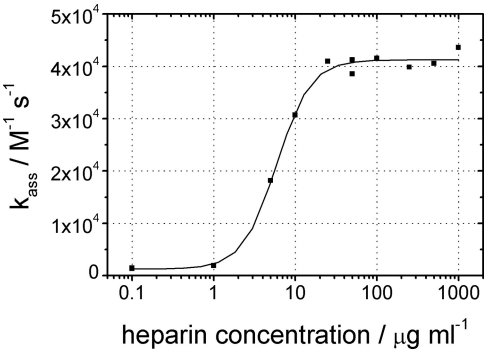

FIGURE 4. The heparin concentration dependence of the acceleration of the AT-MASP-1 reaction by unfractionated heparin at 200 nM AT concentration.

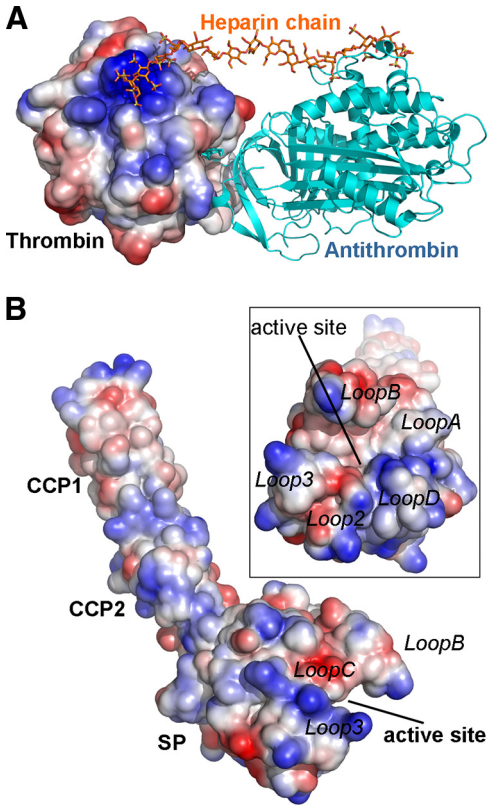

FIGURE 5. Surface electrostatics of MASP-1 compared with the thrombin-heparin-AT ternary complex in search for possible heparin binding sites. *A*, The thrombin-heparin-AT complex with the highly positive heparin binding site of thrombin (PDB id: 1tb6; solvent accessible surface colored for electrostatic potential; red, negative; blue, positive). *B*, MASP-1, shown in similar orientation as thrombin, possesses no significant clustering of positive charges. This suggests there is no high-affinity preformed binding site for heparin on MASP-1, and if there is any it is likely to be different from that of thrombin. *Inset:* No clustering of positive charges can be detected near the substrate binding region of MASP-1, which is the supposed heparin binding region of other proteases in protease-C1-inh-heparin ternary complexes. This is in line with the observation that heparin has no effect on the MASP-1/C1-inh reaction.

Calculated surface charge map of MASP-1 does not show any highly positive regions similar to the heparin binding site of thrombin (Fig. 5), which is in line with the kinetic data.

Discussion

Because MASP-1 is associated with the pattern recognition molecules (MBL, ficolins) of the lectin pathway, initially it seemed evident that it has complement substrates. However, the only complement component that is cleaved efficiently by MASP-1 is C2 ($k_{cat}/K_m = 3 \times 10^4$ M^{-1} s^{-1}) (4). The catalytic efficiency of C1s and MASP-2 toward C2 is higher by one order of magnitude (4, 5). MASP-1 also cleaves C3, but the catalytic efficiency of this reaction is very low (300 M^{-1} s^{-1}), raising doubt on the physiological relevance of this reaction (4, 14). In contrast, MASP-1 cleaves hydrolyzed C3 more efficiently. MASP-1 itself is capable of autoactivation and further autolysis in the SP domain after Arg504 (4). The fact that the catalytic power of MASP-1 is low toward complement substrates (except for C2), and that MASP-1 alone may not initiate the complement cascade, indicates that MASP-1 could have substrates outside the complement system. Indeed, MASP-1 has thrombin-like properties, because it can cleave fibrinogen (α- and β-chains), factor XIII (16, 17), and the protease activated receptor-4 (M. Megyeri, V. Mako, L. Beinrohr, Z. Doleschall, Z. Prohaszka, L. Cervenak, P. Závodszky, P. Gál, unpublished data), and it can be inhibited by AT in the presence of heparin (15).

In this study, quantitative characterization revealed that AT inhibits rMASP-1 both in the presence and absence of heparin. Heparin accelerated the reaction by ~30-fold, which makes AT in the presence of heparin a more potent inhibitor of MASP-1 than C1-inh. In our experiments, the catalytic fragment of MASP-1 was used. Full length MASP-1 in blood is present in a dimeric form associated with MBL or ficolins, which may influence the reactions of MASP-1. The extent of this effect, however, is possibly similar to different serpins. Both serpins (AT and C1-inh) are found in blood at similarly high concentration (2–3 μM), therefore the determined inhibition rates serve as a good indication of their relative contribution to MASP-1 regulation. The fact that AT in the presence of heparin is the most potent inhibitor of MASP-1 found so far reinforces its analogous role with coagulation proteases.

The structure of the ternary complex of thrombin, AT, and heparin (44, 45) confirmed that bridging plays the pivotal role in the heparin acceleration of the thrombin/AT reaction. Thrombin possesses a heparin-binding exosite that is characterized by a cluster of positively charged side chains. The surface electrostatics of MASP-1 do not show any marked, positively charged patches that could constitute a similar, strong heparin binding site. The effect of heparin on C1-inh is characterized by a charge neutralization, or sandwich mechanism (46, 47). Depending on the charge of the protease near the active site, heparin can increase or decrease the rate of inhibition. MASP-1 seems to be neutral in this respect, i.e., heparin does not enhance or reduce the rate of inhibition by C1-inh. These data, along with the kinetic results and the lack of influence of heparin on rMASP-1's activity (data not shown), suggest that heparin does not bind to MASP-1 and acceleration of the MASP-1/AT reaction by heparin is caused by allosteric effects on AT.

It has been shown that the proteolytic activity of MASP-1 can be detected on gelatin zymography, which also indicates broader substrate specificity than a typical complement protease (48). The broad substrate specificity of MASP-1 is reflected in the wide substrate-binding groove in the surface representation of SP domain structure. The opening readily accommodates peptides and hence the surface loops of protein substrates can easily gain access to the active site. In this respect, MASP-1 mostly resembles trypsin among the examined proteases (C1r, C1s, MASP-2, thrombin, and trypsin).

Several lines of evidence indicate that the SP domain of MASP-1 has different evolutionary status than that of the remaining members of the C1r/C1s/MASP family. The members of the S1 peptidase family usually contain three highly conserved disulfide bridges. However, in the cases of C1r, C1s, MASP-2, and MASP-3, the Cys42-Cys58 (chymotrypsin numbering) disulfide bridge, the so-called histidine loop, is missing. Because MASP-1 SP contains the histidine loop, MASP-1 can represent an earlier evolutionary stage of complement SP domains (18). Another important fact that suggests an evolutionary different status is that the SP domain of MASP-1 is encoded by six exons, whereas the SP domain of C1r, C1s, MASP-2, and MASP-3 is encoded by one. One of the evolutionary markers of serine proteases introduced by Krem and Di Cera (49) also show that MASP-1 has a more ancient configuration than the other early complement proteases. MASP-1 has a TCN-encoded active Ser, whereas in the related proteases an AGY codon is found. The evolutionary markers place the SP domain of MASP-1 somewhere between trypsin and thrombin and further apart from C1r, C1s, MASP-2, and MASP-3.

MASP-1's unique features among complement proteases with the same domain organization are reflected in the crystal structure of its catalytic region. The SP domain resembles that of trypsin more than any of those in the MASP-2, C1r, C1s group, hence MASP-1 can be considered as a relatively unspecific protease domain joined to five complement regulatory domains. Of course, MASP-1 is less active and has a more restricted specificity than trypsin, because a protease like that would be unfavorable in blood. In the structure of the SP domain of MASP-1, there are two features that can counteract the impact of the wide substrate-binding groove. One is the unusually large Loop B (also called 60-loop), which might restrict the specificity, and the other is a salt bridge between the crucial Asp residue at the bottom of the S1 pocket and an Arg side chain, which may contribute to the moderate activity of MASP-1 compared with trypsin. A similar salt bridge is involved in the self-inhibitory mechanism that reduces the activity of factor D, the initiator protease of the alternative pathway activation (39, 50, 51). The residue involved in factor D (Arg218) is in the vicinity, but not in equivalent position with the residue (Arg677, c224) in MASP-1. In contrast, factor D has numerous other structural deviations, which render it a practically inactive protease on small substrates. Interestingly, in triple mutant factor D, which has increased activity compared with wild type, Arg223 replaces Arg218 as the partner of Asp189 (50). In this mutant factor D, as well as in MASP-1, the rotation of only a few torsion angles is enough to allow substrate binding. Therefore, the effect of Arg223 in factor D, or Arg677 (c224) in MASP-1 is to reduce, but not to prevent the activity of the protease.

MASP-1 has several substrates outside the complement system, which might contribute to mounting an even more powerful response against infection. In this respect, it is intriguing that MASP-1 is able to cleave protease activated receptor-4, which triggers proinflammatory reactions in leukocytes and endothelial cells (M. Megyeri, V. Mako, L. Beinrohr, Z. Doleschall, Z. Prohaszka, L. Cervenak, P. Závodszky, P. Gál, unpublished data). Our structure explains why MASP-1 behaves as a promiscuous protease compared with the other complement proteases. Its substrate binding groove is quite accessible, resembling that of trypsin; however its reactivity could be modulated by an unusually large loop B (60-loop), and a salt bridge between the S1 Asp and an Arg side chain.

Acknowledgments

We thank István Szabó for his help with the purification of R504Q rMASP-1 and Júlia Balczer for her technical assistance. We thank Dr. Michele Cianti (EMBL, Hamburg, Germany) for help during data collection. Access to EMBL beamline X11 at the DORIS storage ring, DESY, Hamburg is gratefully acknowledged.

Disclosures

J.D., V.H., P.Z., and P.G. have a pending patent regarding the structure. The other authors have no financial conflict of interest.

References

1. Walport, M. J. 2001. Complement: first of two parts. *N. Engl. J. Med.* 344: 1058–1066.
2. Thiel, S. 2007. Complement activating soluble pattern recognition molecules with collagen-like regions, mannan-binding lectin, ficolins and associated proteins. *Mol. Immunol.* 44: 3875–3888.
3. Chen, C. B., and R. Wallis. 2001. Stoichiometry of complexes between mannose-binding protein and its associated serine proteases: defining functional units for complement activation. *J. Biol. Chem.* 276: 25894–25902.
4. Ambrus, G., P. Gál, M. Kojima, K. Szilágyi, J. Balczer, J. Antal, L. Gráf, A. Laich, B. E. Moffatt, W. Schwaeble, R. B. Sim, and P. Závodszky. 2003. Natural substrates and inhibitors of mannan-binding lectin-associated serine protease-1 and -2: a study on recombinant catalytic fragments. *J. Immunol.* 170: 1374–1382.
5. Rossi, V., S. Cseh, I. Bally, N. M. Thielens, J. C. Jensenius, and G. J. Arlaud. 2001. Substrate specificities of recombinant mannan-binding lectin-associated serine proteases-1 and -2. *J. Biol. Chem.* 276: 40880–40887.
6. Dahl, M. R., S. Thiel, M. Matsushita, T. Fujita, A. C. Willis, T. Christensen, T. Vorup-Jensen, and J. C. Jensenius. 2001. MASP-3 and its association with distinct complexes of the mannan-binding lectin complement activation pathway. *Immunity* 15: 127–135.
7. Terai, I., K. Kobayashi, M. Matsushita, and T. Fujita. 1997. Human serum mannose-binding lectin (MBL)-associated serine protease-1 (MASP-1): determination of levels in body fluids and identification of two forms in serum. *Clin. Exp. Immunol.* 110: 317–323.
8. Møller-Kristensen, M., J. C. Jensenius, L. Jensen, N. Thielens, V. Rossi, G. Arlaud, and S. Thiel. 2003. Levels of mannan-binding lectin-associated serine protease-2 in healthy individuals. *J. Immunol. Methods* 282: 159–167.
9. Chen, C. B., and R. Wallis. 2004. Two mechanisms for mannose-binding protein modulation of the activity of its associated serine proteases. *J. Biol. Chem.* 279: 26058–26065.
10. Møller-Kristensen, M., S. Thiel, A. Sjöholm, M. Matsushita, and J. C. Jensenius. 2006. Cooperation between MASP-1 and MASP-2 in the generation of C3 convertase through the MBL pathway. *Int. Immunol.* 19: 141–149.
11. Rawal, N., R. Rajagopalan, and V. P. Salvi. 2008. Activation of complement component C5: comparison of C5 convertases of the lectin pathway and classical pathway of complement. *J. Biol. Chem.* 283: 7853–7863.
12. Takahashi, M., D. Iwaki, K. Kanno, Y. Ishida, J. Xiong, M. Matsushita, Y. Endo, S. Miura, N. Ishii, K. Sugamura, and T. Fujita. 2008. Mannose-binding lectin (MBL)-associated serine protease (MASP)-1 contributes to activation of the lectin complement pathway. *J. Immunol.* 180: 6132–6138.
13. Gál, P., V. Harmat, A. Kocsis, T. Bián, L. Barna, G. Ambrus, B. Végh, J. Balczer, R. B. Sim, G. Náray-Szabó, and P. Závodszky. 2005. A true autoactivating enzyme: structural insights into mannose-binding lectin-associated serine protease-2 activation. *J. Biol. Chem.* 280: 33435–33444.
14. Matsushita, M., S. Thiel, J. C. Jensenius, I. Terai, and T. Fujita. 2000. Proteolytic activities of two types of mannose-binding lectin-associated serine protease. *J. Immunol.* 165: 2637–2642.
15. Presanis, J. S., K. Hajela, G. Ambrus, P. Gál, and R. B. Sim. 2003. Differential substrate and inhibitor profiles for human MASP-1 and MASP-2. *Mol. Immunol.* 40: 921–929.
16. Hajela, K., M. Kojima, G. Ambrus, K. N. H. Wong, B. E. Moffatt, J. Fergula, S. Hajela, P. Gál, and R. B. Sim. 2002. The biological functions of MBL-associated serine proteases (MASPs). *Immunobiology.* 205: 467–475.
17. Krarup, A., K. C. Gulla, P. Gál, K. Hajela, and R. B. Sim. 2008. The action of MBL-associated serine protease 1 (MASP1) on factor XIII and fibrinogen. *Biochim. Biophys. Acta* 1784: 1294–1300.
18. Endo, Y., M. Takahashi, M. Nakao, H. Saiga, H. Sekine, M. Matsushita, M. Nonaka, and T. Fujita. 1998. Two lineages of mannose-binding lectin-associated serine protease (MASP) in vertebrates. *J. Immunol.* 161: 4924–4930.
19. Ricklin, D., and J. D. Lambris. 2007. Complement-targeted therapeutics. *Nat. Biotechnol.* 25: 1265–1275.
20. Walsh, M. C., T. Bourcier, K. Takahashi, L. Shi, M. N. Busche, R. P. Rother, S. D. Solomon, R. A. B. Ezekowitz, and G. L. Stahl. 2005. Mannose-binding lectin is a regulator of inflammation that accompanies myocardial ischemia and reperfusion injury. *J. Immunol.* 175: 541–546.
21. Budayova-Spano, M., M. Lacroix, N. M. Thielens, G. J. Arlaud, J. C. Fontecilla-Camps, and C. Gaboriaud. 2002. The crystal structure of the zymogen catalytic domain of complement protease C1r reveals that a disruptive mechanical stress is required to trigger activation of the C1 complex. *EMBO J.* 21: 231–239.
22. Budayova-Spano, M., W. Grabarse, N. M. Thielens, H. Hillen, M. Lacroix, M. Schmidt, J. C. Fontecilla-Camps, G. J. Arlaud, and C. Gaboriaud. 2002. Monomeric structures of the zymogen and active catalytic domain of complement protease C1r: further insights into the C1 activation mechanism. *Structure* 10: 1509–1519.
23. Kardos, J., V. Harmat, A. Palló, O. Barabás, K. Szilágyi, L. Gráf, G. Náray-Szabó, Y. Goto, P. Závodszky, and P. Gál. 2008. Revisiting the mechanism of the autoactivation of the complement protease C1r in the C1 complex: structure of the active catalytic region of C1r. *Mol. Immunol.* 45: 1752–1760.
24. Gaboriaud, C., V. Rossi, I. Bally, G. J. Arlaud, and J. C. Fontecilla-Camps. 2000. Crystal structure of the catalytic domain of human complement C1s: a serine protease with a handle. *EMBO J.* 19: 1755–1765.
25. Harmat, V., P. Gál, J. Kardos, K. Szilágyi, G. Ambrus, B. Végh, G. Náray-Szabó, and P. Závodszky. 2004. The structure of MBL-associated serine protease-2 reveals that identical substrate specificities of C1s and MASP-2 are realized through different sets of enzyme-substrate interaction. *J. Mol. Biol.* 342: 1533–1546.
26. Gregory, L. A., N. M. Thielens, G. J. Arlaud, J. C. Fontecilla-Camps, and C. Gaboriaud. 2003. X-ray structure of the Ca2+-binding interaction domain of C1s. *J. Biol. Chem.* 278: 32157–32164.
27. Feinberg, H., C. M. Uitdehaag, J. M. Davies, R. Wallis, K. Drickamer, and W. I. Weis. 2003. Crystal structure of the CUB1-EGF-CUB2 region of mannose-binding protein associated serine protease-2. *EMBO J.* 22: 2348–2359.
28. Teillet, F., C. Gaboriaud, M. Lacroix, L. Martin, G. J. Arlaud, and N. M. Thielens. 2008. Crystal structure of the CUB1-EGF-CUB2 domain of human MASP-1/3 and identification of its interaction sites with mannan-binding lectin and ficolins. *J. Biol. Chem.* 283: 25715–25724.

29. Dobó, J., V. Harmat, E. Sebestyén, L. Beinrohr, P. Závodszky, and P. Gál. 2008. Purification, crystallization and preliminary X-ray analysis of human mannose-binding lectin-associated serine protease-1 (MASP-1) catalytic region. *Acta Crystallogr. F.* 64: 781–784.
30. Kabsch, W. 1993. Automatic processing of rotation diffraction data from crystals of initially unknown symmetry and cell constants. *J. Appl. Crystallogr.* 26: 795–800.
31. Vagin, A., and A. Teplyakov. 1997. MOLREP: an automated program for molecular replacement. *J. Appl. Crystallogr.* 30: 1022–1025.
32. Emsley, P., and K. Cowtan. 2004. Coot: model-building tools for molecular graphics. *Acta Crystallogr. D.* 60: 2126–2132.
33. Murshudov, G. N., A. A. Vagin, and E. J. Dodson. 1997. Refinement of macromolecular structures by the maximum-likelihood method. *Acta Crystallogr. D.* 53: 240–255.
34. Laskowski, R. A., M. W. MacArthur, D. S. Moss, and J. M. Thornton. 1993. PROCHECK: a program to check the stereochemical quality of protein structures. *J. Appl. Crystallogr.* 26: 283–291.
35. Kerr, F. K., A. R. Thomas, L. C. Wijeyewickrema, J. C. Whisstock, S. E. Boyd, D. Kaiserman, A. Y. Matthews, P. I. Bird, N. M. Thielens, V. Rossi, and R. N. Pike. 2008. Elucidation of the substrate specificity of the MASP-2 protease of the lectin complement pathway and identification of the enzyme as a major physiological target of the serpin C1-inhibitor. *Mol. Immunol.* 45: 670–677.
36. Dobó, J., and P. G. W. Gettins. 2004. α1-proteinase inhibitor forms initial non-covalent and final covalent complexes with elastase analogously to other serpin-proteinase pairs, suggesting a common mechanism of inhibition. *J. Biol. Chem.* 279: 9264–9269.
37. Schechter, N. M., and M. I. Plotnick. 2004. Measurement of the kinetic parameters mediating protease-serpin inhibition. *Methods* 32: 159–168.
38. Perona, J. J., and C. S. Craik. 1997. Evolutionary divergence of substrate specificity within the chymotrypsin-like serine protease fold. *J. Biol. Chem.* 272: 29987–29990.
39. Narayana, S. V. L., M. Carson, O. El-Kabbani, J. M. Kilpatrick, D. Moore, X. Chen, C. E. Bugg, J. E. Volanakis, and L. J. DeLucas. 1994. Structure of human factor D: a complement system protein at 2.0 Å resolution. *J. Mol. Biol.* 235: 695–708.
40. Wong, N. K., M. Kojima, J. Dobó, G. Ambrus, and R. B. Sim. 1999. Activities of the MBL-associated serine proteases (MASPs) and their regulation by natural inhibitors. *Mol. Immunol.* 36: 853–861.
41. Olson, S. T., I. Björk, R. Sheffer, P. A. Craig, J. D. Shore, and J. Choay. 1992. Role of the antithrombin-binding pentasaccharide in heparin acceleration of antithrombin-proteinase reactions: resolution of the antithrombin conformational change contribution to heparin rate enhancement. *J. Biol. Chem.* 267: 12528–12538.
42. Streusand, V. J., I. Björk, P. G. W. Gettins, M. Petitou, and S. T. Olson. 1995. Mechanism of acceleration of antithrombin-proteinase reactions by low affinity heparin: role of the antithrombin binding pentasaccharide in heparin rate enhancement. *J. Biol. Chem.* 270: 9043–9051.
43. Gettins, P. G. W. 2002. Serpin structure, mechanism, and function. *Chem. Rev.* 102: 4751–4804.
44. Dementiev, A., M. Petitou, J-M. Herbert, and P. G. W. Gettins. 2004. The ternary complex of antithrombin-anhydrothrombin-heparin reveals the basis of inhibitor specificity. *Nat. Struct. Mol. Biol.* 11: 863–867.
45. Li, W., D. J. Johnson, C. T. Esmon, and J. A. Huntington. 2004. Structure of the antithrombin-thrombin-heparin ternary complex reveals the antithrombotic mechanism of heparin. *Nat. Struct. Mol. Biol.* 11: 857–862.
46. Beinrohr, L., V. Harmat, J. Dobó, Z. Lörincz, P. Gál, and P. Závodszky. 2007. C1-inhibitor serpin domain structure reveals the likely mechanism of heparin potentiation and conformational disease. *J. Biol. Chem.* 282: 21100–21109.
47. Beinrohr, L., J. Dobó, P. Závodszky, and P. Gál. 2008. C1, MBL-MASPs and C1-inhibitor: novel approaches for targeting complement-mediated inflammation. *Trends Mol. Med.* 14: 511–521.
48. Gál, P., L. Barna, A. Kocsis, and P. Závodszky. 2007. Serine proteases of the classical and lectin pathways: similarities and differences. *Immunobiology* 212: 267–277.
49. Krem, M. M., and E. Di Cera. 2001. Molecular markers of serine protease evolution. *EMBO J.* 20: 3036–3045.
50. Kim, S., S. V. L. Narayana, and J. E. Volanakis. 1995. Crystal structure of a complement factor D mutant expressing enhanced catalytic activity. *J. Biol. Chem.* 270: 24399–24405.
51. Jing, H., K. J. Macon, D. Moore, L. J. DeLucas, J. E. Volanakis, and S. V. L. Narayana. 1999. Structural basis of profactor D activation: from a highly flexible zymogen to a novel self-inhibited serine protease, complement factor D. *EMBO J.* 18: 804–814.